

Diffusion dynamics of supercooled water modeled with the cage-jump motion and hydrogen-bond rearrangement

Takuma Kikutsuji,¹ Kang Kim,^{1,2, a)} and Nobuyuki Matubayasi^{1,3, b)}

¹⁾Division of Chemical Engineering, Graduate School of Engineering Science, Osaka University, Toyonaka, Osaka 560-8531, Japan

²⁾Institute for Molecular Science, Okazaki, Aichi 444-8585, Japan

³⁾Elements Strategy Initiative for Catalysts and Batteries, Kyoto University, Katsura, Kyoto 615-8520, Japan

(Dated: 20 January 2022)

The slow dynamics of glass-forming liquids is generally ascribed to the cage-jump motion. In the cage-jump picture, a molecule remains in a cage formed by neighboring molecules, and after a sufficiently long time, it jumps to escape from the original position by cage-breaking. The clarification of the cage-jump motion is therefore linked to unraveling the fundamental element of the slow dynamics. Here, we develop a cage-jump model for the dynamics of supercooled water. The caged and jumping states of a water molecule are introduced with respect to the hydrogen-bond (H-bond) rearrangement process, and describe the motion in supercooled states. It is then demonstrated from the molecular dynamics simulation of the TIP4P/2005 model that the characteristic length and time scales of cage-jump motions provide a good description of the self-diffusion constant that is determined in turn from the long-time behavior of the mean square displacement. Our cage-jump model thus enables to connect between H-bond dynamics and molecular diffusivity.

I. INTRODUCTION

The origin of slow dynamics observed in many supercooled liquids below their melting temperatures is frequently explained utilizing the cage-effect picture.^{1,2} This picture advocates that a molecule in supercooled liquids is trapped in the cage transiently formed by neighboring molecules and exhibits escape jump motions due to the cage-breaking after a sufficient long time. The cage-jump scenario also suggests intermittent molecular motions, which can be modeled by the continuous-time random walk using a random waiting time between cage-jumps.³ The cage-jump motion in glassy dynamics has been extensively addressed with molecular dynamics (MD) simulations^{4–17} and experiments using colloidal glasses.^{18–25}

As the temperature is decreased, the mean square displacement (MSD) exhibits a plateau in the intermediate time scales between ballistic and diffusive regimes, reflecting the localized motion inside the cage. This MSD plateau value is associated with the so-called Debye-Waller factor to characterize the degree of localization. However, it is often delicate to quantify the length and time scales of the cage effect from an MD trajectory, which is continuous in space and time and is generated through thermal fluctuations. The cage-jump model adopts a discretized view and introduces the caged and jumping states along the dynamics of a single molecule.

Pastore *et al.* have recently developed a cage-jump model to predict the long-time diffusivity from the short-time cage dynamics in supercooled liquids.^{26–31} In the study, a trajectory of a single particle is segmented into

caged and jumping states. The segmentation criterion was given by the MSD plateau value. Remarkably, the evaluations of jumping length and duration time enabled to estimate the self-diffusion constant that is determined from the MSD long-time behavior at any temperature. This cage-jump modeling demonstrates that the underlying mechanism of the molecular diffusivity is essentially governed by the accumulation of successive cage-jump events.

The aim of this study is to develop a cage-jump model for supercooled water in strong connection to the dynamics of hydrogen-bond (H-bond) network. At normal liquid states, it has been widely accepted that a defect of 3- or 5-coordinated H-bond plays a crucial role for characterizing the H-bond breakage.^{32–34} By contrast, the number of defects decreases when liquid water is supercooled. Correspondingly, the tetrahedrality of H-bond network becomes significant, where the molecular motion is expected to be described by the cage-jump scenario. Indeed, there have been various MD results showing the plateau in MSD of supercooled water.^{35–40} The intermittent jump motions have also been illustrated in supercooled water by analyzing the trajectory of a single molecule.³⁷ In particular, the connection of H-bond rearrangements with the jump motions has been examined.

We have recently revealed that the H-bond lifetime τ_{HB} depends on the temperature in inverse proportion to the self-diffusion constant D .⁴⁰ This result was explained by the correlation between H-bond breakages and translational molecular jumps. Moreover, we have also examined the pathways of hydrogen-bond breakages on the profile of the two-dimensional potential of mean force.⁴¹ It has been clarified that H-bonds break due to translational, rather than rotational motions of the molecules, particularly at supercooled states. Although these studies suggest the strong relationship between the H-bond

^{a)}Electronic mail: kk@cheng.es.osaka-u.ac.jp

^{b)}Electronic mail: nobuyuki@cheng.es.osaka-u.ac.jp

dynamics and molecular diffusivity in liquid water, the connection between the microscopic change of the H-bond network and molecular displacement remains elusive.

The cage-jump model for supercooled water in the present work is established by analyzing the H-bond dynamics. In particular, the caged and jumping states are introduced from the rearrangement process of four-coordinated H-bonds. Thus, our cage-jump model does not rely on a dynamical criterion such as the MSD plateau value. We examine how the H-bond rearrangement process links to the long-time diffusivity.

II. MODEL AND SIMULATIONS

MD simulations were performed using the TIP4P/2005 water model.⁴² All the simulations in this work were performed with the GROMACS2016.4 package.^{43,44} The phase diagram of the TIP4P/2005 supercooled water was determined in Refs. 45 and 46. The temperature crossing the Widom line in the ρ - T phase diagram is $T_L \approx 210$ K at 1 g/cm³. Furthermore, the mode-coupling glass transition is estimated as $T_C \approx 190$ K at 1 g/cm³ in Refs. 47 and 48. Recent MD simulations have reported that the divergence of the structural relaxation time occurs at $T_g \approx 136$ K under the constant 1 bar condition.^{49,50} As described next, we examined the systems close to T_L , while our simulation temperatures are above T_C and T_g .

The mass density was fixed at 1 g/cm³ and the simulation system contained $N = 8,000$ molecules in a cubic box with the periodic boundary conditions. The cell length was approximately $L = 6.2$ nm. The investigated temperatures were $T = 350, 320, 300, 280, 260, 240, 220, 210, 200$, and 190 K. At each temperature, the system was equilibrated for 10 ns in the NVT ensemble, followed by a production run in NVE for 20 ns. Other trajectories of 100 ns were generated for MSD and H-bond correlation function (see the definitions below) at temperatures 200 K and 190 K. A time step of 1 fs was used. As demonstrated below, this trajectory duration is larger than the H-bond lifetime τ_{HB} at all the temperatures examined. Furthermore, aging effects have not been detected in the course of MD simulations. The atomic coordinates were stored at 0.2 ps intervals, which were used for the analyses presented below. This interval was chosen as a time scale slightly larger than that of libration motions (~ 0.1 ps).

The MSD, $\langle \delta r^2(t) \rangle = \langle \sum_{i=1}^N |\Delta \mathbf{r}_i(t)|^2 \rangle / N$, was calculated to quantify the self-diffusion constant D . Here, $\Delta \mathbf{r}_i(t)$ represents the displacement vector of an O atom of the molecule i between two times 0 and t . The results at various temperatures are shown in the inset of Fig. 4(b). At temperatures below 280 K, a plateau becomes noticeable during the intermediate times between ballistic and diffusive regimes, indicating the cage effect. The self-diffusion constant D was determined from the long-time behavior of the MSD, $D = \lim_{t \rightarrow \infty} \langle \delta r^2(t) \rangle / 6t$.

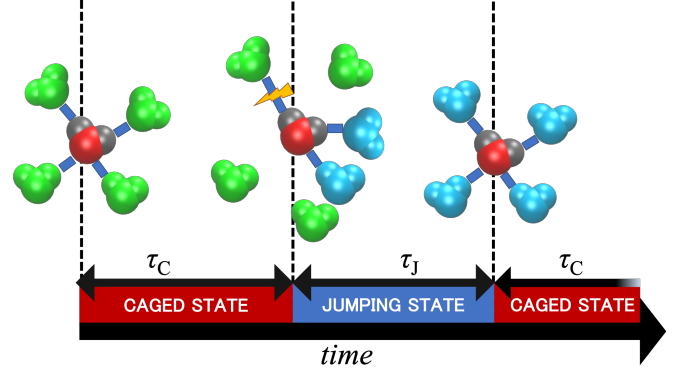


FIG. 1. Schematic illustration to distinguish the caged (C) and jumping (J) states for a tagged water molecule (gray color). The tagged water molecule are H-bonded with neighboring four water molecules (green color), during which the state is labeled as a C state. At a certain point of time, all of four H-bonds are broken and the C state is switched to the J state. After a period of time, the tagged molecule are H-bonded with completely different four water molecules (cyan color), at which the state is switched to the next C state. The duration times of the J and C states are denoted as τ_J and τ_C , respectively.

The ratio of the Lennard-Jones diameter of TIP4P/2005 model and the unit cell is $\sigma/L \approx 0.05$, which is sufficiently small to eliminate the finite-size effect on the diffusion constant.⁵¹

The H-bond was defined using geometric variables between two water molecules. We adopted O-O distance R and OH-O angle β .⁵² Two water molecules are considered H-bonded if the distance-angle relationship meets the condition, $(R, \beta) \leq (0.34 \text{ nm}, 30^\circ)$. The H-bond correlation function $c(t) = \langle h(0)h(t) \rangle / \langle h(0) \rangle$ was calculated with the H-bond indicator $h(t)$ at a time t .^{53,54} It analyzes ‘history-independent’ H-bond correlations, in the sense that $h(t)$ is evaluated only from the configuration at time t without taking into account the reformation of the H-bond in the interval between times 0 and t . The H-bond lifetime τ_{HB} was then determined from $c(t)$ by fitting it to the stretched-exponential function $\exp[-(t/\tau_{HB})^\beta]$.

We classify the time course of each water molecule into two states. One is called caged (C) state, where the tagged water molecule is initially H-bonded to other four water molecules. The schematic illustration of the J and C states is given in Fig. 1. Since an H-bond is of finite lifetime, the four H-bonds with the tagged molecule are all broken at a certain time. This time is set to the start of the jumping (J) state. The next C state then begins at the formation of four H-bonds with water molecules that are totally different from those in the previous C state. The complete changes of the H-bond partners is the con-

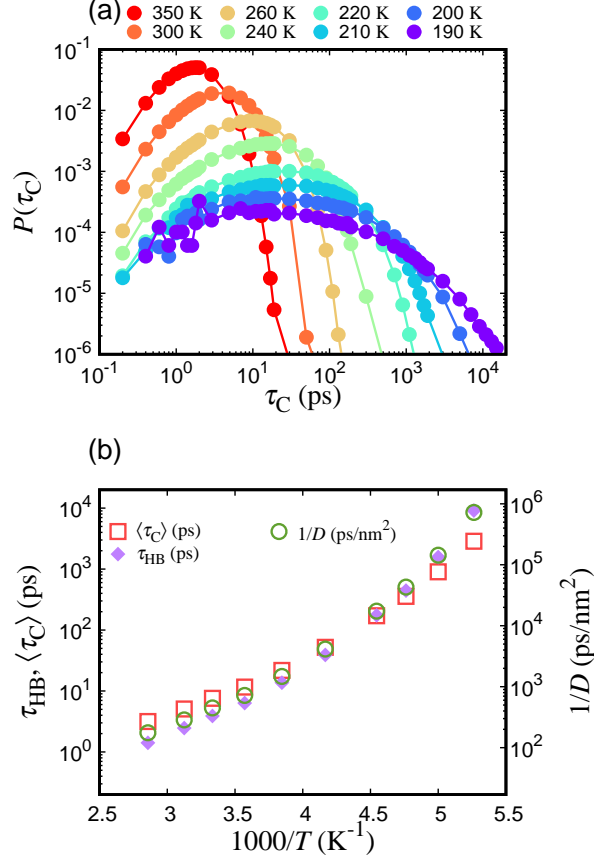


FIG. 2. (a) Distribution of the duration time of the C state, $P(\tau_C)$, at the temperatures examined. (b) Average duration time $\langle\tau_C\rangle$ (left axis), H-bond lifetime τ_{HB} (left axis), and inverse of self-diffusion constant D^{-1} (right axis), as a function of the inverse of the temperature, $1000/T$.

dition of transition from one C state to the next. The end time of a C state is when the four H-bonds are first broken, and the start time is when new, four bonds are formed. The adjacent C states are bridged by a J state, and by definition, a C state may be of 1, 2, 3 or 4 H-bonds and a J state may experience the reformation of an H-bond that was present in the previous C state. When an H-bond in the previous C state reforms after all the four bonds are once broken, the tagged molecule is still in the J state. The duration times of the C and J states are denoted as τ_C and τ_J , respectively. We also quantified the displacement vectors of the O atom of the molecule i during the J state, which is represented as $\Delta\mathbf{r}_i^J(\theta)$. Here, θ is the counter for molecule i to stay at J states from the initial time of the trajectory. Furthermore, many τ_C and τ_J were obtained for the single-molecule trajectory of each water molecule. The averages of τ_C and τ_J over all the single-molecule trajectories are denoted as $\langle\tau_C\rangle$ and $\langle\tau_J\rangle$, respectively. On the other hand, the sum of τ_J along a single trajectory was obtained and its ratio to the total

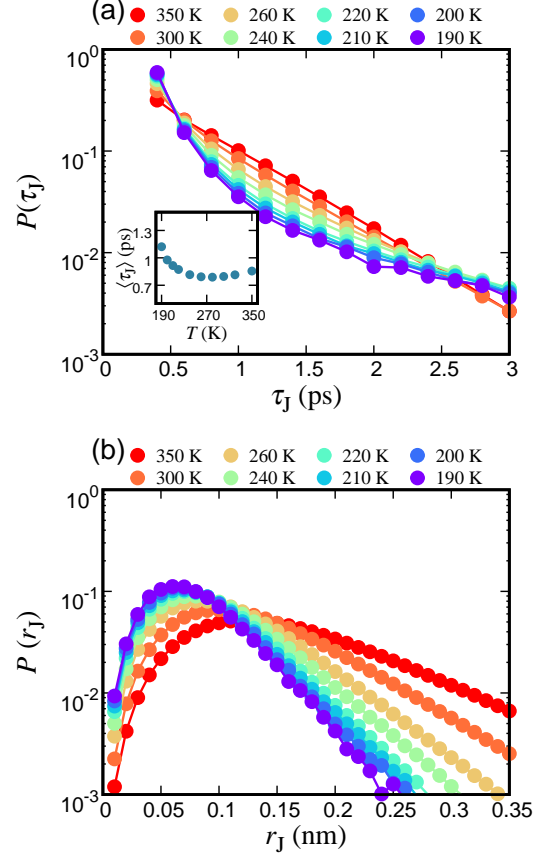


FIG. 3. (a) Distribution of the duration time of the J state, $P(\tau_J)$, at the temperatures examined. Inset: temperature dependence of average jump time $\langle\tau_J\rangle$. (b) Distribution of the jumping length during the jumping state, $P(r_J)$, at the temperatures examined.

length of that trajectory was also determined. The average of this ratio over all the single-molecule trajectories is then called ρ_J . Due to the difference in the order of averaging, ρ_J is in principle different from $\langle\tau_J\rangle/(\langle\tau_C\rangle + \langle\tau_J\rangle)$; this point will be examined at the end of Sec. III. These quantities provide time coarse-grained information filtering out the thermal fluctuations within the J states as well as the libration motions.

III. RESULTS AND DISCUSSION

Figure 2(a) shows the distribution of the duration time of the C state, $P(\tau_C)$, at the temperatures examined. The peak of $P(\tau_C)$ appears at around 10 ps at 300 K, which shifts to time scale of 50 ps at 190 K. In addition, the distribution is gradually extended to slower time scales with decreasing the temperature. The temperature dependence of the average duration time $\langle\tau_C\rangle$ is plotted in Fig. 2(b). In comparison, the temperature

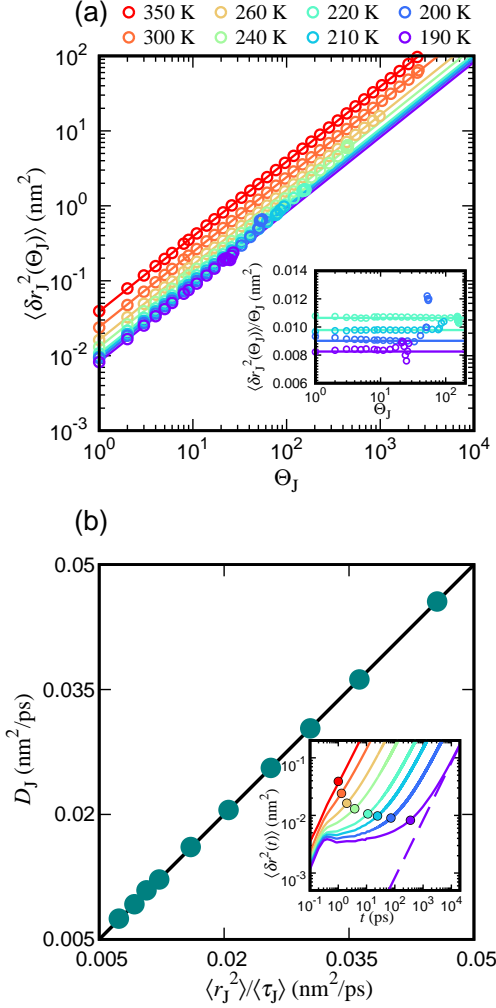


FIG. 4. (a) Jumping mean square displacement (JMSD), $\langle \delta r_J^2(t) \rangle$, as a function of the number of jumps Θ_J at the temperatures examined. Inset: $\langle \delta r_J^2(t) \rangle / \Theta_J$ as a function of Θ_J at temperatures below $T = 200$ K. The straight lines indicate the diffusion behavior, of which slope gives a jumping self-diffusion constant D_J . (b) Jumping self-diffusion constant D_J vs. $\langle r_J^2 \rangle / \langle \tau_J \rangle$ obtained from $P(\tau_J)$ and $P(r_J)$. The black line represents $D_J = \langle r_J^2 \rangle / \langle \tau_J \rangle$. Inset: Mean square displacement (MSD), $\langle \delta r^2(t) \rangle$, at the temperatures examined. Dashed line represents the long-time asymptote $6Dt$ at $T = 190$ K. Points indicate values of the average jump length $\langle r_J^2 \rangle$ at each temperature.

dependence of τ_{HB} and D^{-1} is also plotted in Fig. 2(b). It is demonstrated that the time scales of $\langle \tau_C \rangle$ is akin to τ_{HB} , although the temperature dependence is slightly different. Note that the mean value of H-bond number depends on the temperature ranging from 3.62 at 300 K to 3.97 at 190 K, presumably resulting in the difference between $\langle \tau_C \rangle$ and τ_{HB} . Furthermore, the intimate connection between self-diffusion constant D and H-bond lifetime τ_{HB} is clarified in Fig. 2(b), which is equivalent to

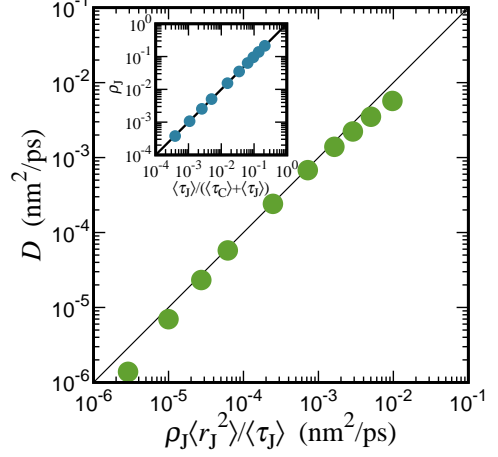


FIG. 5. Self-diffusion constant D vs. the estimate from the cage-jump model $\rho_J \langle r_J^2 \rangle / \langle \tau_J \rangle$. The black line represents $D = \rho_J \langle r_J^2 \rangle / \langle \tau_J \rangle$. Inset: Ratio of jumping state ρ_J vs. the ratio of average jumping time $\langle \tau_J \rangle / (\langle \tau_C \rangle + \langle \tau_J \rangle)$. The black line represents $\rho_J = \langle \tau_J \rangle / (\langle \tau_C \rangle + \langle \tau_J \rangle)$.

the previous demonstration, $D \propto \tau_{HB}^{-1}$, in TIP4P/2005 supercooled water.⁴⁰ The roles of $\langle \tau_C \rangle$ and τ_{HB} for the cage-jump model will be discussed later.

Figure 3(a) shows the distribution of the duration time of the J state, $P(\tau_J)$. Contrary to $P(\tau_C)$ in Fig. 2, the temperature dependence of $P(\tau_J)$ is much smaller. This causes the very weak temperature dependence of the average jumping time $\langle \tau_J \rangle \approx 1$ ps, as seen in the inset of Fig. 3(a). Figure 3(b) shows the distribution of the jumping length during the J state, $P(r_J)$ with $r_J = |\Delta \mathbf{r}_i^J|$. This demonstrates that the peak position length scale of $P(r_J)$ becomes smaller as the temperature is decreased. Furthermore, the exponential decay of $P(r_J)$ beyond the peak position is clearly observed at each temperature. Our results of $P(\tau_J)$ and $P(r_J)$ are compatible with those of supercooled liquid using simple potentials.²⁶ Note that these distributions $P(\tau_J)$ and $P(r_J)$ are sufficiently converged when plenty of jump events are accumulated, requiring times exceeding $\langle \tau_C \rangle$ and τ_{HB} .

We calculated the jumping mean square displacement (JMSD),

$$\langle \delta r_J^2(\Theta_J) \rangle = \frac{1}{N_J} \sum_{i=1}^{N_J} \sum_{\theta=1}^{\Theta_J} |\Delta \mathbf{r}_i^J(\theta)|^2, \quad (1)$$

where Θ_J is the total number of J states during an MD trajectory of a single water molecule. In addition, N_J denotes the number of molecules exhibiting Θ_J jumps in the course of the trajectory. Figure 4(a) shows that the JMSD $\langle \delta r_J^2(\Theta_J) \rangle$ is linear with Θ_J at each temperature. However, we observed some deviations in the JMSD, particularly for larger Θ_J at lower temperatures (see the inset of Fig. 4(a)). These de-

viations from the linearity at large Θ_J are due to the fact that N_J becomes much smaller than N , leading to the insufficient ensemble average over the molecules. At 190 K, for example, N_J becomes smaller than N at $\Theta_J \gtrsim 10$. The average self-diffusion constant D_J of successive jumping events is determined from the relation, $D_J = \lim_{\Theta_J \rightarrow \infty} \langle \delta r_J^2(\Theta_J) \rangle / (\Theta_J \langle \tau_J \rangle)$, where the linear fit was done by excluding the $N_J < N$ regions. Figure 4(b) demonstrates that the second-order moment $\langle r_J^2 \rangle$ of the distribution $P(r_J)$ provides the good description of D_J at each temperature. As discussed in Ref. 26, these features of the JMSD and D_J indicate that the diffusion process of a single molecule can be described by the random walk with independent jumps, which is characterized by $\langle r_J^2 \rangle$. Furthermore, the decrease in D_J with the temperature reduction is attributed to the corresponding decrease in the jumping length scale $\langle r_J^2 \rangle$. The inset of Fig. 4(b) illustrates the location of $\langle r_J^2 \rangle$ in the MSD. At each temperature, the value of $\langle r_J^2 \rangle$ slightly exceeds beyond the MSD plateau. This observation indicates the validity of our modeling for cage-jump motions.

The relevance of the cage-jump modeling is examined in Fig. 5 by plotting the relationship between the self-diffusion constant D and $\rho_J D_J = \rho_J \langle r_J^2 \rangle / \langle \tau_J \rangle$. Note that the inset of Fig. 5 demonstrates the ratio of the J state ρ_J is essentially equal to the ratio of the average jumping time $\langle \tau_J \rangle / (\langle \tau_C \rangle + \langle \tau_J \rangle)$. A similar result was also reported in Ref. 26. It should be noted that ρ_J is obtained by first analyzing each single-molecule trajectory and then taking an average over all the single-molecule trajectories, while $\langle \tau_J \rangle$ and $\langle \tau_C \rangle$ are computed without distinguishing the trajectories of distinct water molecules. $\rho_J = \langle \tau_J \rangle / (\langle \tau_C \rangle + \langle \tau_J \rangle)$ thus implies the validity of a mean-field-type view in that the average over the single-molecule trajectories can be determined without taking into account the differences among the trajectories. Figure 5 shows that $\rho_J D_J$ from our cage-jump model is a good indicator for the self-diffusion constant D , although slight deviations are apparent at 190 K and higher temperatures above 300 K. As shown in Fig. 2(b), the inverse of the self-diffusion constant D^{-1} is strongly coupled with τ_{HB} , which becomes slightly larger than $\langle \tau_C \rangle$. When $\langle \tau_J \rangle \ll \langle \tau_C \rangle$, $\rho_J D_J$ is approximated by $\langle r_J^2 \rangle / \langle \tau_C \rangle$, which holds particularly at lower temperatures. Thus, the difference between $\langle \tau_C \rangle$ and τ_{HB} results in the small difference between D and $\rho_J D_J$ at 190 K. The deviations at high temperatures are attributed to the observation that the MSD plateau was not well developed, as shown in the inset of Fig. 4(b). In fact, at higher temperatures, the cage structures are weakened and water molecules immediately diffuse without exhibiting intermittent cage-jump motions.

IV. CONCLUSIONS

In this paper, we have developed a cage-jump model for the diffusion in supercooled water. Unlike the scheme

proposed by Pastore *et al.*,^{26–31} we classify the trajectory of a single water molecule into the caged and jumping states from the analysis of H-bond rearrangements. The quantification of the average length and time scales of the jumping state enabled to predict the self-diffusion constant D that is determined in principle from the long-time MSD behavior. We have thus succeeded in connecting the H-bond dynamics and the molecular diffusivity through the cage-jump events. This cage-jump event can be regarded as an element of the collective motions, which are often visualized by string-like motions.³⁷ In fact, the time scale is $\langle \tau_J \rangle \approx 1$ ps, whereas that of collective motions is typically characterized by the time of the last stage in the MSD plateau.

Our cage-jump model gives an estimate of D when the caged and jumping states are identified from an MD trajectory, without extensive MSD evaluation to the diffusive regime. In fact, the diffusion asymptote $6Dt$ is observed at times much larger than τ_{HB} , as shown in the inset of Fig. 4(b). However, particularly at lower temperatures, the duration time of the C state $\langle \tau_C \rangle$ becomes slightly smaller than the H-bond lifetime τ_{HB} . This causes the small difference between D and $\rho_J D_J$, particularly at 190 K, as observed in Fig. 5. The local structure changes from high-density liquid to low-density liquid with decreasing the temperature below the so-called Widom line ($T_L \approx 210$ K). The tetrahedral order becomes higher and the number of the defect correspondingly decreases in the low-density liquid state, where the hydrogen-bond break needs more activation energy, and correspondingly the H-bond network rearranges over a wider range in space. In contrast, our cage-jump model is constructed based on the information on the first nearest neighbor shell only. This leads to the underestimation of $\langle \tau_C \rangle$ compared with τ_{HB} . A possible refinement is thus to incorporate order parameters for H-bond network such as the local structure index^{49,55–58}, which focus on the second nearest neighbor. In this respect, further study is currently undertaken toward the appropriate inference of the self-diffusion constant D , particularly at much deeper supercooled states inside the so-called no man's land region.^{49,50,59–61} It is also worthy to apply our cage-jump model to various water models to give deeper insight into the role of the H-bond breakage on the molecular diffusivity in supercooled water.

ACKNOWLEDGMENTS

The authors thank S. Saito and T. Kawasaki for helpful discussions. This work was supported by JSPS KAKENHI Grant Numbers JP18H01188 (K.K.), JP15K13550 (N.M.), and JP19H04206 (N.M.). This work was also supported in part by the Post-K Supercomputing Project and the Elements Strategy Initiative for Catalysts and Batteries from the Ministry of Education, Culture, Sports, Science, and Technology. The numerical calculations were performed at Research Center of Compu-

tational Science, Okazaki Research Facilities, National Institutes of Natural Sciences, Japan.

- ¹C. A. Angell, "Formation of Glasses from Liquids and Biopolymers," *Science* **267**, 1924–1935 (1995).
- ²W. Gotze, "Recent tests of the mode-coupling theory for glassy dynamics," *J. Phys.: Condens. Matter* **11**, A1–A45 (1999).
- ³E. W. Montroll and G. H. Weiss, "Random Walks on Lattices. II," *J. Math. Phys.* **6**, 167–181 (1965).
- ⁴M. M. Hurley and P. Harrowell, "Kinetic structure of a two-dimensional liquid," *Phys. Rev. E* **52**, 1694–1698 (1995).
- ⁵B. Doliwa and A. Heuer, "Cage Effect, Local Anisotropies, and Dynamic Heterogeneities at the Glass Transition: A Computer Study of Hard Spheres," *Phys. Rev. Lett.* **80**, 4915 (1998).
- ⁶R. Yamamoto and A. Onuki, "Dynamics of highly supercooled liquids: Heterogeneity, rheology, and diffusion," *Phys. Rev. E* **58**, 3515–3529 (1998).
- ⁷K. Vollmayr-Lee, "Single particle jumps in a binary Lennard-Jones system below the glass transition," *J. Chem. Phys.* **121**, 4781 (2004).
- ⁸L. Berthier, D. Chandler, and J. P. Garrahan, "Length scale for the onset of Fickian diffusion in supercooled liquids," *EPL* **69**, 320 (2005).
- ⁹P. Chaudhuri, L. Berthier, and W. Kob, "Universal Nature of Particle Displacements close to Glass and Jamming Transitions," *Phys. Rev. Lett.* **99**, 060604 (2007).
- ¹⁰E. J. Saltzman and K. S. Schweizer, "Large-amplitude jumps and non-Gaussian dynamics in highly concentrated hard sphere fluids," *Phys. Rev. E* **77**, 051504 (2008).
- ¹¹R. Candelier, A. W. Cooper, J. K. Kummerfeld, O. Dauchot, G. Biroli, P. Harrowell, and D. R. Reichman, "Spatiotemporal Hierarchy of Relaxation Events, Dynamical Heterogeneities, and Structural Reorganization in a Supercooled Liquid," *Phys. Rev. Lett.* **105**, 135702 (2010).
- ¹²H. Shiba, T. Kawasaki, and A. Onuki, "Relationship between bond-breakage correlations and four-point correlations in heterogeneous glassy dynamics: configuration changes and vibration modes," *Phys. Rev. E* **86**, 041504 (2012).
- ¹³T. Kawasaki and A. Onuki, "Slow relaxations and stringlike jump motions in fragile glass-forming liquids: Breakdown of the Stokes-Einstein relation," *Phys. Rev. E* **87**, 012312 (2013).
- ¹⁴F. W. Starr, J. F. Douglas, and S. Sastry, "The relationship of dynamical heterogeneity to the Adam-Gibbs and random first-order transition theories of glass formation," *J. Chem. Phys.* **138**, 12A541 (2013).
- ¹⁵F. Puosi, C. De Michele, and D. Leporini, "Scaling between relaxation, transport and caged dynamics in a binary mixture on a per-component basis," *J. Chem. Phys.* **138**, 12A532 (2013).
- ¹⁶J. Helfferich, F. Ziebert, S. Frey, H. Meyer, J. Farago, A. Blumen, and J. Baschnagel, "Continuous-time random-walk approach to supercooled liquids. I. Different definitions of particle jumps and their consequences," *Phys. Rev. E* **89**, 042603 (2014).
- ¹⁷J.-H. Hung, T. K. Patra, V. Meenakshisundaram, J. H. Mangalala, and D. S. Simmons, "Universal localization transition accompanying glass formation: insights from efficient molecular dynamics simulations of diverse supercooled liquids," *Soft Matter* **410**, 259 (2019).
- ¹⁸P. N. Pusey and W. van Meegen, "Observation of a glass transition in suspensions of spherical colloidal particles," *Phys. Rev. Lett.* **59**, 2083–2086 (1987).
- ¹⁹A. Kasper, E. Bartsch, and H. Sillescu, "Self-Diffusion in Concentrated Colloid Suspensions Studied by Digital Video Microscopy of Core-Shell Tracer Particles," *Langmuir* **14**, 5004–5010 (1998).
- ²⁰A. H. Marcus, J. Schofield, and S. A. Rice, "Experimental observations of non-Gaussian behavior and stringlike cooperative dynamics in concentrated quasi-two-dimensional colloidal liquids," *Phys. Rev. E* **60**, 5725–5736 (1999).
- ²¹W. K. Kegel and A. van Blaaderen, "Direct Observation of Dynamical Heterogeneities in Colloidal Hard-Sphere Suspensions," *Science* **287**, 290–293 (2000).
- ²²E. R. Weeks, J. Crocker, A. C. Levitt, A. Schofield, and D. Weitz, "Three-Dimensional Direct Imaging of Structural Relaxation Near the Colloidal Glass Transition," *Science* **287**, 627–631 (2000).
- ²³E. R. Weeks and D. A. Weitz, "Properties of Cage Rearrangements Observed near the Colloidal Glass Transition," *Phys. Rev. Lett.* **89**, 095704 (2002).
- ²⁴E. R. Weeks and D. A. Weitz, "Subdiffusion and the cage effect studied near the colloidal glass transition," *Chem. Phys.* **284**, 361–367 (2002).
- ²⁵W. van Meegen and H. J. Schöpe, "The cage effect in systems of hard spheres," *J. Chem. Phys.* **146**, 104503 (2017).
- ²⁶R. Pastore, A. Coniglio, and M. Pica Ciamarra, "From cage-jump motion to macroscopic diffusion in supercooled liquids," *Soft Matter* **10**, 5724–5728 (2014).
- ²⁷R. Pastore, A. Coniglio, and M. P. Ciamarra, "Dynamic phase coexistence in glass-forming liquids," *Sci. Rep.* **5**, 2827 (2015).
- ²⁸R. Pastore, A. Coniglio, and M. P. Ciamarra, "Spatial correlations of elementary relaxation events in glass-forming liquids," *Soft Matter* **11**, 7214–7218 (2015).
- ²⁹M. P. Ciamarra, R. Pastore, and A. Coniglio, "Particle jumps in structural glasses," *Soft Matter* **12**, 358–366 (2016).
- ³⁰R. Pastore, A. Coniglio, A. de Candia, A. Fierro, and M. Pica Ciamarra, "Cage-jump motion reveals universal dynamics and non-universal structural features in glass forming liquids," *J. Stat. Mech.* **2016**, 054050 (2016).
- ³¹R. Pastore, G. Pesce, A. Sasso, and M. Pica Ciamarra, "Cage Size and Jump Precursors in Glass-Forming Liquids: Experiment and Simulations," *J. Phys. Chem. Lett.* **8**, 1562–1568 (2017).
- ³²D. Laage and J. T. Hynes, "A Molecular Jump Mechanism of Water Reorientation," *Science* **311**, 832–835 (2006).
- ³³D. Laage and J. T. Hynes, "On the Molecular Mechanism of Water Reorientation," *J. Phys. Chem. B* **112**, 14230–14242 (2008).
- ³⁴G. Stirnemann and D. Laage, "Communication: On the origin of the non-Arrhenius behavior in water reorientation dynamics," *J. Chem. Phys.* **137**, 031101 (2012).
- ³⁵F. Sciortino, P. Gallo, P. Tartaglia, and S. H. Chen, "Supercooled water and the kinetic glass transition," *Phys. Rev. E* **54**, 6331–6343 (1996).
- ³⁶P. Gallo, F. Sciortino, P. Tartaglia, and S. H. Chen, "Slow Dynamics of Water Molecules in Supercooled States," *Phys. Rev. Lett.* **76**, 2730–2733 (1996).
- ³⁷N. Giovambattista, M. G. Mazza, S. V. Buldyrev, F. W. Starr, and H. E. Stanley, "Dynamic Heterogeneities in Supercooled Water," *J. Phys. Chem. B* **108**, 6655–6662 (2004).
- ³⁸N. Giovambattista, S. V. Buldyrev, H. E. Stanley, and F. W. Starr, "Clusters of mobile molecules in supercooled water," *Phys. Rev. E* **72**, 011202 (2005).
- ³⁹P. Gallo and M. Rovere, "Mode coupling and fragile to strong transition in supercooled TIP4P water," *J. Chem. Phys.* **137**, 164503 (2012).
- ⁴⁰T. Kawasaki and K. Kim, "Identifying time scales for violation/preservation of Stokes-Einstein relation in supercooled water," *Sci. Adv.* **3**, e1700399 (2017).
- ⁴¹T. Kikutsuji, K. Kim, and N. Matubayasi, "How do hydrogen bonds break in supercooled water?: Detecting pathways not going through saddle point of two-dimensional potential of mean force," *J. Chem. Phys.* **148**, 244501 (2018).
- ⁴²J. L. F. Abascal and C. Vega, "A general purpose model for the condensed phases of water: TIP4P/2005," *J. Chem. Phys.* **123**, 234505 (2005).
- ⁴³B. Hess, C. Kutzner, D. van der Spoel, and E. Lindahl, "GROMACS 4: Algorithms for Highly Efficient, Load-Balanced, and Scalable Molecular Simulation," *J. Chem. Theory Comput.* **4**, 435–447 (2008).
- ⁴⁴M. J. Abraham, T. Murtola, R. Schulz, S. Páll, J. C. Smith, B. Hess, and E. Lindahl, "GROMACS: High performance molecular simulations through multi-level parallelism from laptops to supercomputers," *SoftwareX* **1-2**, 19–25 (2015).
- ⁴⁵R. S. Singh, J. W. Biddle, P. G. Debenedetti, and M. A. Anisi-

- mov, “Two-state thermodynamics and the possibility of a liquid-liquid phase transition in supercooled TIP4P/2005 water,” *J. Chem. Phys.* **144**, 144504 (2016).
- ⁴⁶J. W. Biddle, R. S. Singh, E. M. Sparano, F. Ricci, M. A. Gonzalez, C. Valeriani, J. L. F. Abascal, P. G. Debenedetti, M. A. Anisimov, and F. Caupin, “Two-structure thermodynamics for the TIP4P/2005 model of water covering supercooled and deeply stretched regions,” *J. Chem. Phys.* **146**, 034502 (2017).
- ⁴⁷M. De Marzio, G. Camisasca, M. Rovere, and P. Gallo, “Mode coupling theory and fragile to strong transition in supercooled TIP4P/2005 water,” *J. Chem. Phys.* **144**, 074503 (2016).
- ⁴⁸M. De Marzio, G. Camisasca, M. Rovere, and P. Gallo, “Microscopic origin of the fragile to strong crossover in supercooled water: The role of activated processes,” *J. Chem. Phys.* **146**, 084502 (2017).
- ⁴⁹S. Saito, B. Bagchi, and I. Ohmine, “Crucial role of fragmented and isolated defects in persistent relaxation of deeply supercooled water,” *J. Chem. Phys.* **149**, 124504 (2018).
- ⁵⁰S. Saito and B. Bagchi, “Thermodynamic picture of vitrification of water through complex specific heat and entropy: A journey through “no man’s land,”” *J. Chem. Phys.* **150**, 054502 (2019).
- ⁵¹I.-C. Yeh and G. Hummer, “System-Size Dependence of Diffusion Coefficients and Viscosities from Molecular Dynamics Simulations with Periodic Boundary Conditions,” *J. Phys. Chem. B* **108**, 15873–15879 (2004).
- ⁵²R. Kumar, J. R. Schmidt, and J. L. Skinner, “Hydrogen bonding definitions and dynamics in liquid water,” *J. Chem. Phys.* **126**, 204107 (2007).
- ⁵³A. Luzar and D. Chandler, “Hydrogen-bond kinetics in liquid water,” *Nature* **379**, 55–57 (1996).
- ⁵⁴A. Luzar and D. Chandler, “Effect of Environment on Hydrogen Bond Dynamics in Liquid Water,” *Phys. Rev. Lett.* **76**, 928–931 (1996).
- ⁵⁵E. Shiratani and M. Sasai, “Growth and collapse of structural patterns in the hydrogen bond network in liquid water,” *J. Chem. Phys.* (1996).
- ⁵⁶E. Shiratani and M. Sasai, “Molecular scale precursor of the liquid–liquid phase transition of water,” *J. Chem. Phys.* **108**, 3264–3276 (1998).
- ⁵⁷M. J. Cuthbertson and P. H. Poole, “Mixturelike Behavior Near a Liquid-Liquid Phase Transition in Simulations of Supercooled Water,” *Phys. Rev. Lett.* **106**, 91 (2011).
- ⁵⁸R. Shi and H. Tanaka, “Microscopic structural descriptor of liquid water,” *J. Chem. Phys.* **148**, 124503 (2018).
- ⁵⁹R. Shi, J. Russo, and H. Tanaka, “Origin of the emergent fragile-to-strong transition in supercooled water,” *Proc. Natl. Acad. Sci. U.S.A.* **115**, 9444–9449 (2018).
- ⁶⁰R. Shi, J. Russo, and H. Tanaka, “Common microscopic structural origin for water’s thermodynamic and dynamic anomalies,” *J. Chem. Phys.* **149**, 224502 (2018).
- ⁶¹Y. Ni, N. J. Hestand, and J. L. Skinner, “Communication: Diffusion constant in supercooled water as the Widom line is crossed in no man’s land,” *J. Chem. Phys.* **148**, 191102 (2018).